Solving Highly Detailed Gas Transport MINLPs: Block Separability and Penalty Alternating Direction Methods

Björn Geissler[1], Antonio Morsi[1], Lars Schewe[1], Martin Schmidt[2]

Abstract. Detailed modeling of gas transport problems leads to nonlinear and nonconvex mixed-integer optimization or feasibility models (MINLPs) because both the incorporation of discrete controls of the network as well as accurate physical and technical modeling is required in order to achieve practical solutions. Hence, ignoring certain parts of the physics model is not valid for practice. In the present contribution we extend an approach based on linear relaxations of the underlying nonlinearities by tailored model reformulation techniques yielding block-separable MINLPs. This combination of techniques allows us to apply a penalty alternating direction method and thus to solve highly detailed MINLPs for large-scale real-world instances. The practical strength of the proposed method is demonstrated by a computational study in which we apply the method to instances from steady-state gas transport including both pooling effects with respect to the mixing of gases of different composition and a highly detailed compressor station model.

Optimizing or feasibility testing of a given inflow-outflow-situation in gas transport networks is a mathematically challenging task. Typical models lead to nonconvex mixed-integer nonlinear optimization or feasibility problems (MINLPs) that are very hard to solve for large-scale real-world instances. The mixed-integer aspects of these models are needed for describing discrete controls of devices like (control) valves or compressor stations; see, e.g., [11]. However, even after fixing the discrete decisions, the combination of highly nonlinear gas dynamics in pipes and typically nonlinear as well as nonconvex models of technical entities like, e.g., compressor stations, from the engineering literature already leads to NLP type models that are hard to solve; see, e.g., [35, 36]. For recent surveys of this field of research see, e.g., [19, 28] and the references therein.

Due to its hardness, different approaches have been developed in the recent years for tackling problems from gas transport. One main branch relies on (piecewise) linearization techniques for obtaining mixed-integer linear (MIP) models that can be solved with state-of-the-art MIP solvers; see, e.g., [7–11, 21, 22]. Whereas this approach has the clear advantage in addressing the discrete aspects of the problem it is often problematic to model arbitrary nonlinearities. However, the technical and physical modeling of gas flow and the technical entities of the network is very important for practitioners if they have to rely on the obtained optimization results.

Another branch mainly considers NLP type models that result from fixing all discrete decisions in the network; see, e.g., [35, 36]. Following this approach, it is possible to model (more or less) arbitrary nonlinearities, but discrete decisions are not able to change within these approaches, although there are some MPEC type approaches that try to model the switching of discrete states within continuous

Date: March 2, 2017.

2010 *Mathematics Subject Classification.* 65K10, 90-08, 90B10, 90C06, 90C11, 90C35, 90C90.

Key words and phrases. Nonconvex Mixed-Integer Nonlinear Optimization, Penalty Methods, Alternating Direction Methods, Block Separability, Gas Transport.

models; see, e.g., [1, 27, 32–34]. However, these approaches typically cannot compete with MIP approaches if it comes to more complicated mixed-integer formulations.

As described, there is no generic catch-all approach. This is the reason why a third approach has been studied, namely the combination of MIP and NLP techniques for addressing both complicated discrete structures as well as highly nonlinear aspects; see [4] or the approaches described in [19]. More recently, alternating direction methods (ADMs) have been used to combine mixed-integer and continuous solution strategies in a hybrid approach in [13]. In the case of ADMs, variables and constraints of the original problem are decomposed into blocks and the problem is iteratively solved by only optimizing into the direction of the separate blocks. Classical ADMs are extensions of augmented Lagrangian methods. They are originally proposed in [14] and [6] in the context of nonlinear variational problems. Under mild assumptions on the regularity of the objective function and the constraint set it can be shown that ADMs converge to so-called partial minima. However, stronger convergence results can be obtained under additional assumptions like differentiability of the objective or convexity of the objective and the feasible set. A general presentation of the convergence theory of ADMs based on the augmented Lagrangian (ADMM) can be found in [2]. The special case of ADMs applied to convex objective functions $f(x, y)$ over disjoint constraint sets $x \in X, y \in Y$ is discussed in [39]. An extension to the case of biconvex f is given in [15]. Finally, applications of ADMMs in the broad area of machine learning and the possibility of parallelization of ADMMs is discussed in detail in [3].

In [13] we used an extended penalty framework that encompasses a classical ADM for solving gas transport problems with quality tracking. The incorporation of the latter aspect is important from a practical point of view but leads to additional pooling type constraints that are extremely hard to solve using an "integrated" MINLP model. Thus, the idea was to decompose this aspect from the rest of the model.

In this contribution, we show that graph-based decompositions of the original gas transport MINLP can be developed that allow to reformulate the model such that one obtains a so-called block- or quasi-separable form of the MINLP that can be exploited by ADM approaches; see [26]. This decomposition is carefully chosen such that the decomposition of [13] can still also be used. This allows us to extend the above sketched MIP approach for solving gas transport problems by highly detailed, nonlinear, and nonconvex models for compressor stations. This is of significant practical importance because compressor stations are among the most important controllable entities in gas transport networks. Moreover, it turned out that using less detailed compressor station models, as in [13], the computed solutions are likely to violate the admissible operating ranges of the compressors. By using the penalty ADM motivated in [13] and theoretically and computationally studied in [12] we are now able to solve highly detailed physics and engineering models combined with discrete controls for large-scale real-world networks.

The paper is organized as follows: In Section 1 we briefly review the penalty alternating direction method and state its convergence results from [12]. In Section 2 we then propose an MINLP model of steady-state gas transport including both mixing aspects for different types of gas quality and a highly detailed compressor model. Moreover, we present tailored model reformulations in Section 3 that yield block-separability so that the problem fits into the framework of our method. A computational study for the penalty alternating direction method applied to large-scale real-world gas transport networks is given in Section 4. The paper closes with some concluding remarks in Section 5.

1. The Penalty Alternating Direction Method

In this section we briefly review the penalty alternating direction method (PADM) for solving problems of the type

$$\min_{x,y} \quad f(x,y) \quad \text{s.t.} \quad g(x,y) = 0,\ h(x,y) \geq 0,\ x \in X,\ y \in Y. \tag{1}$$

The idea behind this formulation is that most of the constraints solely restrict x or y and that only few constraints g and h couple these blocks of variables. Thus, this formulation is especially tailored for decomposition approaches if the constraints g and h are low-dimensional. An earlier version of this method has also been used heuristically in [13] for solving simplified (w.r.t. the models discussed in this paper) problems from gas transport to feasibility. In the meantime, we developed a convergence theory for PADM in [12], where the following discussion of the method can be found in more detail.

Throughout the paper, we make the following assumptions on Problem (1):

Assumption 1. *The objective function $f : \mathbb{R}^n \to \mathbb{R}$ and the constraint functions $g : \mathbb{R}^n \to \mathbb{R}^m$, $h : \mathbb{R}^n \to \mathbb{R}^p$ are continuous and the constraint sets X and Y are non-empty and compact.*

In the following, we denote by Ω the feasible set, i.e.,

$$\Omega = \{(x,y) \in X \times Y : g(x,y) = 0,\ h(x,y) \geq 0\}.$$

Before we formally state the penalty ADM, we briefly review standard alternating direction methods. A typical ADM works as follows: Given an iterate (x^k, y^k) it first computes a new x-iterate

$$x^{k+1} \in \arg\min_x \{f(x,y^k) : g(x,y^k) = 0,\ h(x,y^k) \geq 0,\ x \in X\}$$

by solving Problem (1) for y fixed to y^k and then computes a new y-iterate

$$y^{k+1} \in \arg\min_y \{f(x^{k+1},y) : g(x^{k+1},y) = 0,\ h(x^{k+1},y) \geq 0,\ y \in Y\}$$

by solving the problem with x fixed to x^{k+1}. It is shown in the literature that this procedure converges to so-called partial minima of Problem (1).

Definition 1.1 (Partial minimum)**.** A feasible point $(x^*, y^*) \in \Omega$ is called a *partial minimum* of f over Ω, if

$$\begin{aligned} f(x^*,y^*) &\leq f(x,y^*) \quad \text{for all } (x,y^*) \in \Omega, \\ f(x^*,y^*) &\leq f(x^*,y) \quad \text{for all } (x^*,y) \in \Omega. \end{aligned}$$

It holds that a partial minimum is a stationary point if f is continuously differentiable. If f and Ω are additionally convex it is easy to show that partial minimizers are also global minimizers [39]. The most basic convergence result for ADMs can be found, e.g., in [15].

Theorem 1.2. *Let $\{(x^i,y^i)\}_{i=0}^{\infty}$ be a sequence with $(x^{i+1},y^{i+1}) \in \Theta(x^i,y^i)$, where*

$$\Theta(x^i,y^i) := \{(x^*,y^*) : \forall x \in X.\ f(x^*,y^i) \leq f(x,y^i);\ \forall y \in Y.\ f(x^*,y^*) \leq f(x^*,y)\}.$$

Suppose that Assumption 1 holds and that the solution of the first optimization problem is always unique. Then every convergent subsequence of $\{(x^i,y^i)\}_{i=0}^{\infty}$ converges to a partial minimum. For two limit points z, z' of such subsequences it holds that $f(z) = f(z')$.

Algorithm 1 : An ℓ_1 Penalty Alternating Direction Method

Choose initial values $(x^{0,0}, y^{0,0}) \in X \times Y$ and penalty parameters $\mu^0, \rho^0 \geq 0$.
for $k = 0, 1, \ldots$ **do**
  Set $l = 0$.
  while $(x^{k,l}, y^{k,l})$ is not a partial minimum of $(\mathrm{P}_{\mu^k,\rho^k})$ **do**
    Compute $x^{k,l+1} \in \arg\min_x \{\phi_1(x, y^{k,l}; \mu^k, \rho^k) : x \in X\}$.
    Compute $y^{k,l+1} \in \arg\min_y \{\phi_1(x^{k,l+1}, y; \mu^k, \rho^k) : y \in Y\}$.
    Set $l \leftarrow l + 1$.
  Choose new penalty parameters $\mu^{k+1} \geq \mu^k$ and $\rho^{k+1} \geq \rho^k$.

From now on, we present a weighted ℓ_1 penalty method based on the classical ADM framework sketched above. To this end, we define the ℓ_1 penalty function

$$\phi_1(x, y; \mu, \rho) := f(x, y) + \sum_{i=1}^{m} \mu_i \, |g_i(x, y)| + \sum_{i=1}^{p} \rho_i [h_i(x, y)]^-,$$

where

$$[\alpha]^- := \begin{cases} 0, & \text{if } \alpha \geq 0, \\ -\alpha, & \text{if } \alpha < 0, \end{cases}$$

and $\mu = (\mu_i)_{i=1}^m, \rho = (\rho_i)_{i=1}^p \geq 0$ are the penalty parameters for the equality and inequality constraints. Note that we allow for different penalty parameters for the constraints instead of a single penalty parameter as it is often the case for penalty methods.

The penalty ADM now proceeds as follows. Given a starting point and initial values for all penalty parameters, the alternating direction method described above is used to compute a partial minimum of the penalty problem

$$\min_{x,y} \quad \phi_1(x, y; \mu, \rho) \quad \text{s.t.} \quad x \in X, \ y \in Y. \tag{$\mathrm{P}_{\mu,\rho}$}$$

Afterward, the penalty parameters are updated and the next penalty problem is solved to partial optimality. Thus, the algorithm produces a sequence of partial minima of a sequence of penalty problems of type $(\mathrm{P}_{\mu,\rho})$. More formally, the method is specified in Algorithm 1.

We now briefly discuss the convergence results for the penalty ADM (Algorithm 1). To this end, let $\chi_{\mu,\rho}$ be the weighted ℓ_1 feasibility measure of Problem (1), which we define as

$$\chi_{\mu,\rho}(x, y) := \sum_{i=1}^{m} \mu_i \, |g_i(x, y)| + \sum_{i=1}^{p} \rho_i [h_i(x, y)]^-.$$

Obviously, $\chi_{\mu,\rho}(x, y) \geq 0$ holds and $\chi_{\mu,\rho}(x, y) = 0$ if and only if (x, y) is feasible w.r.t. g and h. With this notation we can state the following main convergence theorem.

Theorem 1.3 (Geißler et al. [12])**.** *Suppose that Assumption 1 holds and that $\mu_i^k \nearrow \infty$ for all $i = 1, \ldots, m$ and $\rho_i^k \nearrow \infty$ for all $i = 1, \ldots, p$ are monotonically increasing sequences. Moreover, let (x^k, y^k) be a sequence of partial minima of (P_{μ^k,ρ^k}) generated by Algorithm 1 with $(x^k, y^k) \to (x^*, y^*)$. Then*

a) (x^*, y^*) is a partial minimum of the original problem (1) *or*
b) there exist weights $\bar{\mu}, \bar{\rho} \geq 0$ such that (x^*, y^*) is a partial minimizer of the feasibility measure $\chi_{\bar{\mu},\bar{\rho}}$.

If f is additionally differentiable, then (x^*, y^*) is a stationary point of the original problem (1) *in case a). If in addition the feasible set Ω as well as f over Ω are convex, then (x^*, y^*) is a global optimum of the original problem* (1) *in case a).*

The interpretation of the theorem is as follows: In the positive case (a) the algorithm converges to a partial minimum of the overall problem that is, in particular, a feasible point for the original problem. This especially means that all ℓ_1 penalty terms in ϕ_1 are zero in the limit. However, the latter cannot be guaranteed. In the negative case (b) that corresponds to the case in which not all ℓ_1 penalty terms can be driven to zero, the theorem states that the algorithm then converges to a partial minimizer of the weighted feasibility measure χ.

See [12] for a proof. There it is also shown that it is possible to generalize the classical result on the exactness of the ℓ_1 penalty function (see, e.g., [17] or [25]) to the setting of partial minima; see Theorem 3.5 in [12].

2. The Problem

Our application problem from steady-state gas transport can be summarized as follows: Find values of the controls and states of a gas network such that all physical and technical constraints are satisfied. The basic model for this problem that we describe in Section 2.1 is a variant of the model discussed in [19] and [27]. An extension of the model introducing heat-power supply and demand as presented in [13] is subsequently summarized in Section 2.2. In addition to [13] we model compressor groups and the contained compressors and drives in much more detail. In Section 2.3 we introduce a model of compressor groups, which are small subnetworks that we later use for our model reformulation presented in Section 3.

2.1. Basic Network Model.

The basic model of the gas network we use is described in [27] and [19], see especially the chapters [5] and [31], where a detailed discussion and derivation can be found. The following section gives a self-contained description of the model.

We model a gas network as a finite directed graph $G = (V, A)$ with node set V and arc set A. The set of nodes is partitioned into the set of entry nodes V_+, at which gas is supplied, the set of exit nodes V_-, where gas is withdrawn, and the set of inner nodes V_0. The set of arcs consists of pipes A_{pi}, resistors A_{rs}, valves A_{va}, and control valves A_{cv}. Furthermore, we split the set A_{rs} of resistors into resistors with nonlinear and flow dependent pressure loss ($A_{\text{rs-nl}}$) and those with a constant and only flow sign dependent pressure loss relation ($A_{\text{rs-lin}}$). In addition, we distinguish between automated control valves ($A_{\text{cv-aut}}$) and those with an only manually adjustable preset pressure ($A_{\text{cv-man}}$). Finally, we also consider compressor groups. These groups are subgraphs of the entire network graph and we denote their arc set by A_{cg}. A summary of the components of a gas network is given in Table 1.

Using pressure variables p_u at the nodes and describing the gas flow along arcs of the network as well as the supplied or withdrawn gas at the nodes by the mass flow variables q_a and q_u, respectively, the model introduced in [27] and [19] can be summarized as follows:

$$\begin{aligned}
&\text{Exist} && \text{pressures } p, \text{mass flows } q, \dots \\
&\text{s.t.} && \sum_{a \in \delta^{\text{out}}(u)} q_a - \sum_{a \in \delta^{\text{in}}(u)} q_a = \begin{cases} q_u, & \text{if } u \in V_+ \cup V_-, \\ 0, & \text{if } u \in V_0, \end{cases} && u \in V, && \text{(2a)} \\
& && p_v^2 = c_{1,a} p_u^2 - c_{2,a} \left|q_a\right| q_a, && a = (u,v) \in A_{\text{pi}}, && \text{(2b)} \\
& && p_u^2 - p_v^2 + \left|p_u - p_v\right| (p_u - p_v) = 2 c_a \left|q_a\right| q_a, && a = (u,v) \in A_{\text{rs-nl}}, && \text{(2c)}
\end{aligned}$$

TABLE 1. Gas network components

Network components	Index set
Nodes	V
Entries	V_+
Exits	V_-
Inner nodes	V_0
Arcs	A
Pipes	A_{pi}
Resistors	A_{rs}
nonlinear flow dependent	$A_{\text{rs-nl}}$
constant flow sign dependent	$A_{\text{rs-lin}}$
Valves	A_{va}
Control valves	A_{cv}
automated	$A_{\text{cv-aut}}$
manually adjustable	$A_{\text{cv-man}}$
Compressor groups	A_{cg}
Compressor machines	A_{cm}
Turbo compressors	A_{tc}
Piston compressors	A_{pc}

$$p_u - p_v = \operatorname{sgn}(q_a)\xi_a \approx \begin{cases} \xi_a, & \text{if } q_a \geq \varepsilon, \\ -\xi_a, & \text{if } q_a \leq -\varepsilon, \\ \xi_a q_a/\varepsilon, & \text{otherwise,} \end{cases} \quad a \in A_{\text{rs-lin}}, \tag{2d}$$

$$\begin{cases} a \text{ is open} & \implies p_u = p_v, \\ a \text{ is closed} & \implies q_a = 0, \end{cases} \quad a \in A_{\text{va}}, \tag{2e}$$

$$\begin{cases} a \text{ is active} & \implies \Delta_a^- \leq p_u - p_v \leq \Delta_a^+, \\ a \text{ is closed} & \implies q_a = 0, \end{cases} \quad a = (u,v) \in A_{\text{cv-aut}}, \tag{2f}$$

$$\begin{cases} p_v > p_a^{\text{set}} & \implies q_a = 0, \\ p_v < p_a^{\text{set}} & \implies p_v = p_u, \\ p_v = p_a^{\text{set}} & \implies \begin{array}{l}[(p_u \geq p_a^{\text{set}} \wedge q_a \geq 0)] \\ \vee [q_a = 0 \vee (p_v = p_u)],\end{array} \end{cases} \quad a = (u,v) \in A_{\text{cv-man}}, \tag{2g}$$

$$p_u \in [p_u^-, p_u^+], \quad u \in V, \quad q_u \in [q_u^-, q_u^+], \quad u \in V_+ \cup V_-, \tag{2h}$$

$$q_a \in [q_a^-, q_a^+], \quad a \in A, \tag{2i}$$

$$(p_u, p_v, q_a) \in \Omega_a, \quad a \in A_{\text{cg}}? \tag{2j}$$

All variables used in these constraints or later are summarized in Table 2. All quantities that are not listed in the table are constants in our model. Constraints (2a) describe the mass flow balance at the nodes in terms of Kirchhoff's first law. Here we use the notational convention that flows along arc direction and supplies have positive signs and flows against arc direction and demands are reflected by negative signs. The relation between flow and pressure is given by Constraints (2b) for pipes, by Constraints (2c) for resistors with nonlinear pressure loss relation, and by Constraints (2d) for resistors with only flow sign dependent constant pressure loss ξ_a. The parameters c collect all relevant constants like pipe diameter and roughness or drag factors of resistors; the user-specified constant $\varepsilon > 0$ in (2d) is used for piecewise linear re-modeling of the sign function. The combinatorial behavior of

TABLE 2. Variables of the basic model (top; see Section 2.1), the heat-power extension (middle; see Section 2.2), and the detailed compressor group model (bottom; see Section 2.3)

Symbol	Description	Index set
p_u	Gas pressure	$u \in V$
q_u	Mass flow supply or demand	$u \in V_+ \cup V_-$
q_a	Mass flow	$a \in A$
s_a	Binary decision (e.g., open, active)	$a \in A_{\mathrm{va}} \cup A_{\mathrm{cv}} \cup A_{\mathrm{cg}}$
P_u	Heat-power supply or demand	$u \in V_+ \cup V_-$
$H_{\mathrm{c},u}$	Mixed calorific value	$u \in V$
P_a	Heat-power/energy flow	$a \in A$
$H_{\mathrm{c},a}$	Mixed calorific value	$a \in A$
ρ_a^{in}	density at inlet node u of $a = (u, v)$	$a \in A_{\mathrm{cm}}$
$H_{\mathrm{ad},a}$	Change in specific adiabatic enthalpy	$a \in A_{\mathrm{cm}}$
Q_a	Volumetric flow at inlet operating conditions	$a \in A_{\mathrm{cm}}$
n_a	Compressor speed	$a \in A_{\mathrm{cm}}$
$P_{\mathrm{c},a}$	Power consumption	$a \in A_{\mathrm{cm}}$
$P_{\mathrm{c},a}^+$	Maximum power delivered by drive	$a \in A_{\mathrm{cm}}$
$\eta_{\mathrm{ad},a}$	Adiabatic efficiency	$a \in A_{\mathrm{tc}}$
M_a	Shaft torque	$a \in A_{\mathrm{pc}}$

valves and (non-)automated control valves is described by Constraints (2e)–(2g). In (2f), $\Delta_a^{\pm}$ denotes the lower and upper bound of the pressure reduction at the automated control valve, whereas the preset pressure of non-automated control valves is denoted by p_a^{set}. For corresponding mixed-integer formulations using binary variables s_a for $a \in A_{\mathrm{va}} \cup A_{\mathrm{cv}}$ representing the states (e.g., open, closed, active) we refer to [9].

Finally, the abstract constraint (2j) models the feasibility of a pressure-flow situation at compressor groups. The specific modeling of these groups is more complicated. We describe it in detail in Section 2.3.

2.2. **Heat-Power Supply and Demand.** While mass flow is the natural physical quantity for gas supply and demand, the consideration of supply and demand in terms of heat-power is very important in practice. Therefore the gas composition, and in particular the calorific value of the gas mixture, must be tracked throughout the network. An extension of Model (2) introducing additional calorific value (H_{c}) and heat-power (P; sometimes also denoted as energy flow) variables has been developed in [13]. Using the notation

$$\mathcal{I}(u) := \{a \in \delta^{\mathrm{in}}(u) : q_a \geq 0\} \cup \{a \in \delta^{\mathrm{out}}(u) : q_a \leq 0\},$$
$$\mathcal{O}(u) := \{a \in \delta^{\mathrm{in}}(u) : q_a < 0\} \cup \{a \in \delta^{\mathrm{out}}(u) : q_a > 0\},$$

the model extension can be summarized as follows:

$$P_u = \bar{P}_u, \quad u \in V_+ \cup V_-, \tag{3a}$$

$$P_u = q_u H^{\text{ext}}_{\text{c},u}, \quad u \in V_+, \tag{3b}$$

$$P_u = q_u H_{\text{c},u} \quad u \in V_-, \tag{3c}$$

$$P_a = q_a H_{\text{c},a}, \quad a \in A, \tag{3d}$$

$$H_{\text{c},a} = H_{\text{c},u}, \quad u \in V,\ a \in \mathcal{O}(u), \tag{3e}$$

$$\sum_{a \in \mathcal{O}(u)} |P_a| - \sum_{a \in \mathcal{I}(u)} |P_a| = \begin{cases} P_u, & \text{if } u \in V_+ \cup V_-, \\ 0, & \text{if } u \in V_0, \end{cases} \quad u \in V. \tag{3f}$$

The linear constraints (3a) introduce a fixed heat-power supply and demand. We remark that this assignment could be relaxed to lower and upper bounds on heat-power supply and demand. Constraints (3b) define the heat-power supply as the product of mass flow supply and the calorific value $H^{\text{ext}}_{\text{c},u}$ of the supplied gas. Since the latter is a given constant, these constraints are linear as well. Similarly using the calorific value of the mixed gas at a node or at an arc, the heat-power delivered at a node and the heat-power flow through an arc are defined by Constraints (3c) and (3d), which are quadratic and bilinear constraints that yield nonconvex feasible sets. The mixing behavior at nodes is described by Constraints (3e) and (3f). The two last constraints are genuinely nonsmooth since the sets $\mathcal{I}(u)$ and $\mathcal{O}(u)$ are not known a priori. For a derivation of this model we refer to [13]. We remark that an alternative model for including heat-power flows together with appropriate linearization techniques is given in [38].

2.3. **Compressor Groups.** We now describe compressor groups, i.e., we explain the specific constraints that model the abstract feasible set in (2j). In realistic networks, small groups of compressor machines and drives are hosted together and used in such a way that the gas enters through a single inlet, is routed through a series of parallel compressor machines, and leaves via a single outlet. It is thus a dispatching decision to choose from a predefined subset of series-parallel arrangements, called configurations, of the compressor machines. In addition, it is possible to enable a bypass mode to avoid compression or to choose a shut-off mode to block gas flow. To reflect this behavior in our model, we introduce compressor groups. If the entire compressor group is shut-off it behaves like a closed valve, if it is in bypass mode it behaves like an open valve, and otherwise it is active and exactly one of the possible configurations must be selected. For addressing possible pressure losses due to complex station piping, additional resistor elements are placed at the inlet and outlet of the group. These in- and outlet resistors are modeled as standalone resistors; see Constraints (2c) and (2d). See also [29] for a detailed description of compressor group MINLP models.

In order to be able to model all the mentioned aspects, we represent compressor groups by subgraphs consisting of compressor machines A_{cm}, associated drives that deliver the machines with the required power, and additional valves for modeling station piping, i.e., the choice of the specific configuration to use. An example for such a subgraph of a compressor group with two configurations, arising from series-parallel arrangements of two compressor machines is depicted in Figure 1. We denote the subset of arcs contained in compressor groups by A_{cg}, define $\bar{A}_{\text{cg}} := A \setminus A_{\text{cg}}$, and assume that all compressor machines are part of compressor groups, i.e., $A_{\text{cm}} \subseteq A_{\text{cg}}$. The subset of nodes inside or at the boundary of compressor groups is denoted by

$$V_{\text{cg}} := \{u \in V : a = (u, v) \in A_{\text{cg}} \text{ or } a = (v, u) \in A_{\text{cg}}\},$$

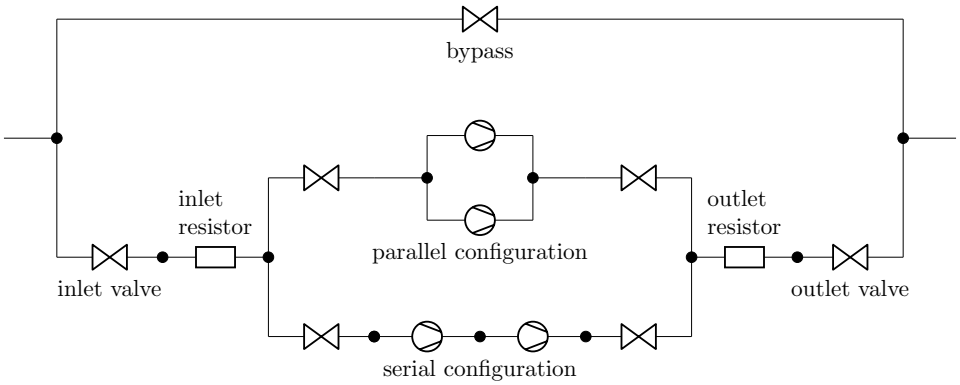

FIGURE 1. Schematic representation of a compressor group subnetwork with two configurations

whereas the subset of nodes outside or at the boundary of compressor groups is given by

$$\bar{V}_{\mathrm{cg}} := \{u \in V : a = (u,v) \in \bar{A}_{\mathrm{cg}} \text{ or } a = (v,u) \in \bar{A}_{\mathrm{cg}}\}.$$

For the ease of presentation and w.l.o.g. we assume that $V_{\mathrm{cg}} \subseteq V_0$ holds. We remark that entities similar to compressor groups are sometimes called compressor stations. However, since realistic stations are more complex—e.g., many stations have more than one inlet and outlet—we follow [19] and use the term "group".

To include more generic technical operating restrictions—even coupling compressor groups, valves, and control valves—we use a generalization of the restricted combinatorial behavior of a compressor group subgraph to arbitrary subgraphs, called subnetwork operation modes. With the concept of subnetwork operation modes it is, e.g., straight forward to reflect the behavior of complex compressor stations or to realize model simplifications like, e.g., symmetry breaking. Here, we refrain from explicitly stating all combinatorial constraints for modeling the (de-)activating of a compressor group or for modeling the choice of a single configuration for an active compressor group (see [13, 19] for the details) but concentrate on the physical and technical models of compressor machines and their associated drives. We distinguish between turbo compressors (A_{tc}) and piston compressors (A_{pc}), i.e., $A_{\mathrm{cm}} = A_{\mathrm{tc}} \cup A_{\mathrm{pc}}$ holds. The full set of technical and physical constraints modeling compressor machines reads

$$H_{\mathrm{ad},a} = c_a \left(\left(\frac{p_v}{p_u} \right)^{\frac{\kappa-1}{\kappa}} - 1 \right) s_a, \quad a \in A_{\mathrm{cm}}, \tag{4a}$$

$$Q_a = (q_a/\rho_a^{\mathrm{in}}) s_a,\ \rho_a^{\mathrm{in}} = p_u/(R_{\mathrm{s}} T z(p_u)), \quad a = (u,v) \in A_{\mathrm{cm}}, \tag{4b}$$

$$H_{\mathrm{ad},a} = F_2(Q_a, n_a; A_a^{H_{\mathrm{ad}}}) s_a,\ \eta_{\mathrm{ad},a} = F_2(Q_a, n_a; A_a^{\eta_{\mathrm{ad}}}) s_a, \quad a \in A_{\mathrm{tc}}, \tag{4c}$$

$$H_{\mathrm{ad},a} \in [F_1(Q_a; b_a^{\mathrm{c}}) s_a,\ F_1(Q_a; b_a^{\mathrm{s}}) s_a],\ n_a \in [n_a^-, n_a^+], \quad a \in A_{\mathrm{tc}}, \tag{4d}$$

$$M_a = \frac{V_{\mathrm{o},a} H_{\mathrm{ad},a}}{2\pi\eta_{\mathrm{ad},a}} \rho_a^{\mathrm{in}} s_a,\ s_a V_{\mathrm{o},a} n_a^- \le Q_a \le s_a V_{\mathrm{o},a} n_a^+, \quad a \in A_{\mathrm{pc}}, \tag{4e}$$

$$0 \le \begin{cases} s_a(\varepsilon_a^+ p_u - p_v) \\ \vee\, s_a(\Delta p_a^+ + p_u - p_v) \\ \vee\, s_a(M_a^+ - M_a), \end{cases} \qquad a \in A_{\mathrm{pc}}. \tag{4f}$$

Constraints (4a) describe the change in specific adiabatic enthalpy $H_{\mathrm{ad},a}$ of the compression process that depends on physical constants c_a and the isentropic exponent κ. The volumetric flow rate Q_a at the inlet of compressor machines is

defined in Constraints (4b) and depends on the gas density ρ_a^{in} at the inlet node. The latter is given by an equation of state for real gas, which is modeled using the compressibility factor z. The binary variable s_a indicates whether the compressor is shut off ($s_a = 0$) or active ($s_a = 1$). The characteristic diagrams of turbo compressors in terms of isolines of speed and isolines of adiabatic efficiency in $(Q_a, H_{\text{ad},a})$-space are given by Constraints (4c). Here $F_2(x, y; A) := (1, x, x^2)A(1, y, y^2)^\top$ denotes a biquadratic polynomial. The coefficient matrix $A \in \mathbb{R}^{3\times 3}$ typically stems from least-squares data fits. Left and right boundaries of characteristic diagrams known as surge- and chokeline are given by Constraints (4d). Lower and upper boundaries are given by lower and upper speed limits $n_a^{\pm}$; see also (4d). Here, $F_1(z; b) := (1, z, z^2)b$ with $b \in \mathbb{R}^3$ is a quadratic polynomial. The feasible operating range of piston compressors is given by Constraints (4e) and (4f) that define characteristic diagrams in (Q_a, M_a)-space, where M_a is the piston compressor's shaft torque. The latter depends on the operating volume $V_{\text{o},a}$ of the piston compressor. Finally, the possible limitations of the operating range of piston compressors are either given by the maximum pressure ratio ε_a^+, the maximum pressure increase Δp_a^+, or the maximum shaft torque M_a^+. The power

$$P_{\text{c},a} = q_a H_{\text{ad},a}/\eta_{\text{ad},a} \tag{5}$$

required for compression depends on the amount of compressed gas in terms of mass flow q_a, the change in specific adiabatic enthalpy $H_{\text{ad},a}$, and the adiabatic efficiency $\eta_{\text{ad},a}$ of the compressor machine $a \in A_{\text{cm}}$. The required energy is delivered by an associated drive. Every drive has a maximum power P_{c}^+ that can be delivered for the compression process. This maximum power depends on the compressor machine's speed n_a and—depending on the specific drive type—on the ambient temperature $T_{\text{amb},a}$. A generic relation for the maximum power of a drive can be stated as a biquadratic polynomial with coefficients obtained from a least-squares data fit:

$$\begin{aligned} P_{\text{c},a} \le P_{\text{c},a}^+ &= P_{\text{c},a}^+(n_a, T_{\text{amb},a}) = F_2(n_a, T_{\text{amb},a}; A_a^{\text{max-power}}) \\ &= (1, n_a, n_a^2)A_a^{\text{max-power}}(1, T_{\text{amb},a}, T_{\text{amb},a}^2)^\top. \end{aligned} \tag{6}$$

Depending on the specific drive, the consumed power is either electricity or gas taken from the network itself as fuel. Electric energy is delivered by specific electric motors, whereas gas is transformed to mechanical energy by gas turbines or gas driven motors. We remark that the above inequality assumes that a drive is associated with exactly one compressor machine. Nonetheless it is straight forward to adapt the inequality to the case where a drive may be connected to multiple compressor machines.

3. Model Summary and ADM Tailored Block-Separable Reformulation

We now collect all variables and constraints discussed in the last section and state the full model. For convenience, all variables required to model compressor groups including compressor machines and drives are collected in the variable vector z from now on. With this notation at hand, the entire model under consideration reads

$$\text{Exists} \quad (p, q, P, H_{\text{c}}, z, s) \quad \text{s.t.} \quad (2)\text{–}(6)? \tag{7}$$

Since the goal of this model is to check whether a given flow-pressure-situation—a so-called nomination—can be transported, we refer to this problem as the problem of validating nominations. Model (7) is a nonlinear and nonconvex mixed-integer feasibility problem. It combines discrete controls of the active network elements with nonlinear pressure loss models, a pooling-type mixing model for gas qualities, and an accurate model of compressor groups including compressors and drives. Thus, it is very hard to solve and cannot be tackled by general-purpose state-of-the-art MINLP solvers on large-scale real-world instances. This is the reason why we develop an

equivalent block-separable reformulation that can be tackled by the penalty ADM of Section 1. Hence, our goal is to achieve a model decomposition of (7) into disjoint and only loosely coupled blocks in order to obtain a model structured as Problem (1).

The main idea is to split all variables and constraints related to compressor groups and all calorific value variables from the basic model. A decomposition into fully disjoint blocks of constraints and variables (like $x \in X$ and $y \in Y$ as in Model (1)) cannot be achieved directly because all compressor group variables and constraints are coupled with the rest of the model by all variables and constraints that are defined on the boundary nodes $V_{\mathrm{cg}} \cap \bar{V}_{\mathrm{cg}}$ of all compressor groups. Thus, to completely fit into the structure of Problem (1), we apply two reformulation steps.

First, we duplicate all coupling pressure variables at nodes incident to—i.e., at the boundary of—compressor groups. This yields new variables p'_u for all $u \in V_{\mathrm{cg}} \cap \bar{V}_{\mathrm{cg}}$. We associate p'_u-variables to compressor group subnetworks and p_u-variables to the remaining network. Next, we have to identify the constraints that couple between blocks; see g, h in Model (1). These coupling constraints are given by $p_u = p'_u$ for all $u \in V_{\mathrm{cg}} \cap \bar{V}_{\mathrm{cg}}$ and their violation will be penalized by ℓ_1 terms

$$f_1 := \left\| (p_u - p'_u)_{u \in V_{\mathrm{cg}} \cap \bar{V}_{\mathrm{cg}}} \right\|_1$$

in the objective function. That is, the new set of variables is finally split up into

$$x = \left((p_u)_{u \in \bar{V}_{\mathrm{cg}}}, (q_u)_{u \in V_+ \cup V_-}, (P_u)_{u \in V_+ \cup V_-}, (q_a, P_a, s_a)_{a \in \bar{A}_{\mathrm{cg}}} \right),$$

$$y = \left((p_u)_{u \in V_{\mathrm{cg}} \setminus \bar{V}_{\mathrm{cg}}}, (p'_u)_{u \in V_{\mathrm{cg}} \cap \bar{V}_{\mathrm{cg}}}, z, (H_{\mathrm{c},u})_{u \in V}, (q_a, P_a, s_a)_{a \in A_{\mathrm{cg}}}, (H_{\mathrm{c},a})_{a \in A} \right).$$

Second, we remove the mass and power flow coupling constraints (2a) and (3f) for all compressor group boundary nodes $u \in V_{\mathrm{cg}} \cap \bar{V}_{\mathrm{cg}}$ from the constraint set and penalize their violation using ℓ_1 objective terms

$$f_2 := \left\| \left(\sum_{a \in \delta^{\mathrm{out}}(u)} q_a - \sum_{a \in \delta^{\mathrm{in}}(u)} q_a \right)_{u \in V_{\mathrm{cg}} \cap \bar{V}_{\mathrm{cg}}} \right\|_1,$$

$$f_3 := \left\| \left(\sum_{a \in \mathcal{O}(u)} |P_a| - \sum_{a \in \mathcal{I}(u)} |P_a| \right)_{u \in V_{\mathrm{cg}} \cap \bar{V}_{\mathrm{cg}}} \right\|_1.$$

By doing so, we have already completely decoupled the compressor group models from the remaining part of the network model.

Lastly, we decouple the relations between mass flows, power flows, and calorific values. In Section 2.2 we have seen that the bilinear constraints (3c) and (3d) make the overall problem much harder to solve. This bilinearity can be used in our ADM setting because fixing either the calorific value or the mass flow (see the definition of x and y above) in these constraints yields simple linear constraints. Thus, we also remove these equations from the constraint set and penalize their violation via

$$f_4 := \left\| (P_a - q_a H_{\mathrm{c},a})_{a \in A} \right\|_1, \quad f_5 := \left\| (P_u - q_u H_{\mathrm{c},u})_{u \in V_-} \right\|_1. \tag{8}$$

See [13] for a more detailed discussion of the latter decomposition.

In summary, we have reformulated Model (7) as

$$\min \quad f_1 + f_2 + f_3 + f_4 + f_5 \quad \text{s.t.} \quad x \in X,\ y \in Y,$$

where X is defined by the Constraints (2a)–(2i) of the basic model and by all heat power constraints (3a), (3b), (3e), (3f) "outside" compressor groups, whereas Y is defined by all compressor group constraints (4) and all heat power constraints (3a), (3b), (3e), (3f) "inside" compressor groups. To summarize, the first-stage ADM model determines values for pressures, mass and heat-power flows, as well as switching

decisions for all elements of the network outside compressor group subnetworks. Pressures, mass and heat-power flows, switching decisions, all compressor and drive specific variable values inside compressor group subnetworks as well as all calorific values throughout the entire network are subsequently computed by solving the second-stage ADM model.

Note again that f_2 and f_3 are the penalizations of Constraints (2a) and (3f) for all nodes $V_{\mathrm{cg}} \cap \bar{V}_{\mathrm{cg}} \subseteq V_0$. This is why these subsets of Constraints (2a) and (3f) are only present in X or Y for nodes $u \notin V_{\mathrm{cg}} \cap \bar{V}_{\mathrm{cg}}$. Nonetheless, we add respective balance constraints that force flow balance of each compressor group subnetwork. For this, let $V_{\mathrm{cg}}^{(i)} \subseteq V_{\mathrm{cg}}$ and $A_{\mathrm{cg}}^{(i)} \subseteq A_{\mathrm{cg}}$ denote the set of all nodes and arcs in compressor group i, respectively. In the first-stage ADM model we add

$$\sum_{u \in V_{\mathrm{cg}}^{(i)} \cap \bar{V}_{\mathrm{cg}}} \left(\sum_{a \in \delta^{\mathrm{out}}(u) \setminus A_{\mathrm{cg}}^{(i)}} q_a - \sum_{a \in \delta^{\mathrm{in}}(u) \setminus A_{\mathrm{cg}}^{(i)}} q_a \right) = 0,$$

$$\sum_{u \in V_{\mathrm{cg}}^{(i)} \cap \bar{V}_{\mathrm{cg}}} \left(\sum_{a \in \mathcal{O}(u) \setminus A_{\mathrm{cg}}^{(i)}} |P_a| - \sum_{a \in \mathcal{I}(u) \setminus A_{\mathrm{cg}}^{(i)}} |P_a| \right) = 0$$

for each compressor group subnetwork i. In the second-stage ADM model we add the equations

$$\sum_{u \in V_{\mathrm{cg}}^{(i)} \cap \bar{V}_{\mathrm{cg}}} \left(\sum_{a \in \delta^{\mathrm{out}}(u) \cap A_{\mathrm{cg}}^{(i)}} q_a - \sum_{a \in \delta^{\mathrm{in}}(u) \cap A_{\mathrm{cg}}^{(i)}} q_a \right) = 0,$$

$$\sum_{u \in V_{\mathrm{cg}}^{(i)} \cap \bar{V}_{\mathrm{cg}}} \left(\sum_{a \in \mathcal{O}(u) \cap A_{\mathrm{cg}}^{(i)}} |P_a| - \sum_{a \in \mathcal{I}(u) \cap A_{\mathrm{cg}}^{(i)}} |P_a| \right) = 0,$$

for each compressor group subnetwork i. These linear combinations of balance equations are added to strengthen the penalty ADM formulation without complicating the solution process at each stage.

There are further important remarks on the proposed second-stage ADM model. As already mentioned, there are no entries inside compressor group subnetworks and gas enters a compressor group through at most one inlet node. This leads to the fact that the problem of computing calorific values is independent from the compressor group subproblems, because at most one type of gas mixture flows through a subnetwork and hence no mixing model is necessary. Moreover, compressor group subnetworks are pairwise disjoint for practically relevant gas networks. Thus, the compressor groups subproblem decomposes into smaller independent optimization problems that can all be solved in parallel. As a consequence, the second-stage ADM model decomposes further into $|A_{\mathrm{cg}}|$ independent compressor group subproblems plus one independent optimization problem for computing updated calorific values. We further remark that the presented block-separable reformulation approach is not restricted to compressor group subnetworks, but could also be applied to arbitrary subnetwork structures.

Let us now finally discuss the types of models that have to be solved within Algorithm 1 after applying the presented reformulations. The first-stage model is still a nonconvex MINLP that we solve using MIP relaxation techniques, see [8–11], that ensure the satisfaction of predefined maximum linearization error tolerances. See [13, 24] for a detailed description of efficient linear relaxation schemes in this context. The compressor group subnetwork models of the second-stage ADM problem are

TABLE 3. Number of nodes and arcs for the L- and H-gas network.

	L-gas	H-gas
Entries	12	45
Exits	964	429
Junctions	3222	2261
Pipes	3899	2258
Resistors	292	557
Valves	401	545
Control valve stations	120	145
Compressor machines	22	104
Compressor groups	12	41

nonconvex mixed-integer nonlinear optimization problems. However, due to our block-separable reformulation, these MINLPs are quite small so that they can be solved by general-purpose state-of-the-art global MINLP solvers. Finally, computing the updated calorific values corresponds to solving a system of linear equations.

4. Computational Results

In this section, we present computational results for two large-scale real-world gas networks that facilitate a detailed discussion of the impact of the fine-grained compressor models presented in Section 2 on the runtime of the overall algorithm. By doing so, we present the first real-world application of the penalty ADM from [12].

We proceed with a brief description of the test instances in Section 4.1 and the computational setup in Section 4.2, before we discuss the impact of the detailed compressor model on the runtime of the algorithm in Section 4.3.

4.1. **Test Instances.** We consider the two major subnetworks of Germany's largest gas transport network operated by our former project partner Open Grid Europe GmbH (OGE)[1]. The first subnetwork is used for the transport of low-calorific gas (L-gas) with calorific values ranging from $34\,\mathrm{MJ/Nm^3}$ to $36\,\mathrm{MJ/Nm^3}$; see Figure 2. The second one is used for the transport of high calorific gas (H-gas) with calorific values from $36\,\mathrm{MJ/Nm^3}$ to $44\,\mathrm{MJ/Nm^3}$; see Figure 3. For the L-gas network we are given 28 and for the H-gas network we are given 30 feasible instances for the problem of validating nominations. These 58 instances are hand-made expert scenarios that have been provided to us by OGE to evaluate our algorithms. The dimensions of the networks are given in Table 3. For further information on the networks we refer to [13].

4.2. **Computational Setup.** All computations presented below have been carried out on a computer with an Intel Core i7-4702HQ processor running at 2.2 GHz and with 16 GB of main memory. All models have been implemented using the C++ framework LaMaTTO++ for modeling and solving mixed-integer nonlinear optimization problems on networks [20]. All MIP and LP models have been solved with Gurobi 6.0.4 [16] using only a single thread and a limit of 2000 branch-and-bound nodes. All MINLP models have been set up with GAMS 24.5.4 [23] and we used Baron 15.6.5 [30, 37] to solve the MINLPs.

Finally, we remark that although it is possible to solve all second-stage ADM models in parallel, we apply a sequential variant for reasons of simplicity of the implementation.

[1] `https://www.open-grid-europe.com`

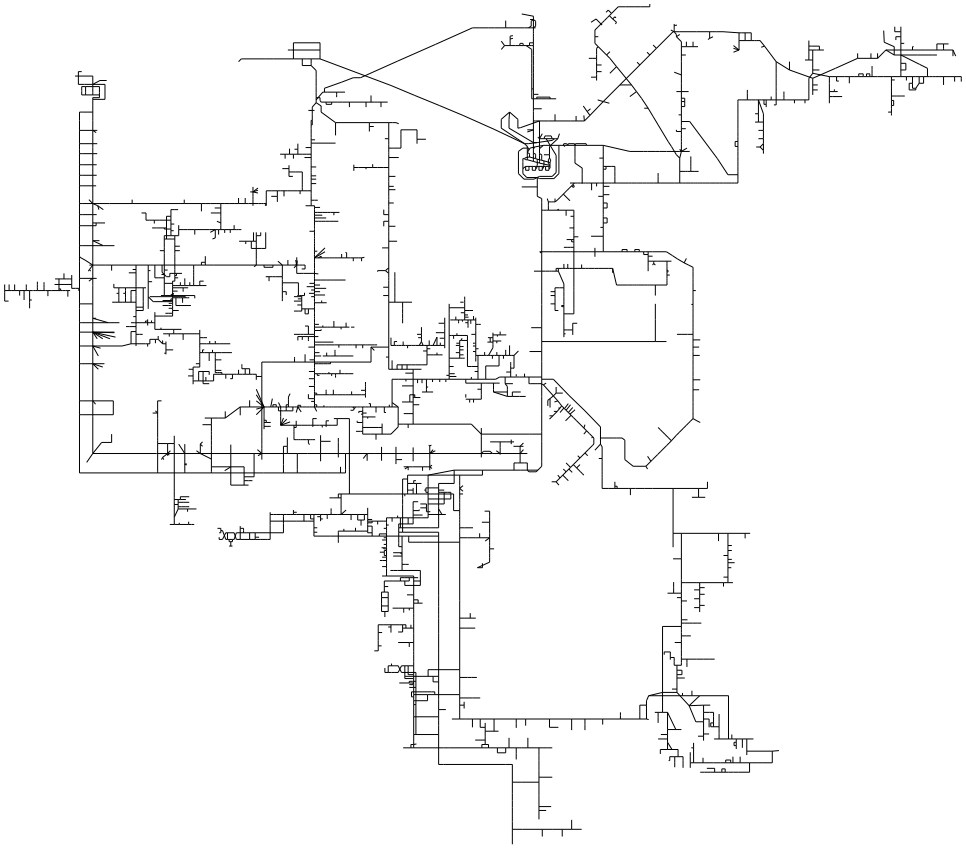

FIGURE 2. Schematic plot of the L-gas network.

4.3. **Discussion.** In this section, we compare the runtime of our algorithm for the case with the relaxed compressor model used in [13], where the restrictions of drives are omitted and where the operating ranges of the compressor machines are convexified, with the runtimes of our algorithm for Model (7) from Section 2 with nonconvex operating ranges and the full nonlinear drive model. By doing so, we can measure the influence of more detailed compressor models on the runtimes of the penalty ADM.

We have to point out that Algorithm 1, applied to the relaxed model from [13], alternatingly solves MIP and LP subproblems, whereas applying Algorithm 1 to Problem (7) additionally requires to solve an MINLP subproblem for each compressor group in each ADM iteration.

Before we discuss the numerical results in detail we have to comment on two implementation details. First, we slightly modify the first-stage ADM model w.r.t. the model described in Section 3. During our numerical experiments, it turned out that it is favorable to extend the first-stage model by a linear relaxation of the second-stage compressor model. This does not harm the theoretical analysis of the penalty ADM but leads to a stronger similarity of the compressor model of the first and second stage and, thus, to less effort for the penalty framework for coupling the block-separated parts of the decomposed model; see, in particular, the ℓ_1 penalty terms f_1, f_2, and f_3. Therefore the nonconvex operating range of a turbo compressor, see (4c)–(4d), is replaced by a convex superset and during branch-and-bound, we cut off any point outside this convexified operating range by a separating hyperplane.

This relaxation is the same as the one used in [13]. Its derivation and a detailed description can be found in [9]. Second, our experiments suggest to apply only a single ADM iteration per penalty iteration instead of computing a partial minimum of the penalty problems in each penalty iteration.

The results for the L-gas network are presented in Table 4. For the H-gas network the results are summarized in Table 5. The columns headed by "simplified" contain the results for the simplified compressor model from [13], while the columns headed by "detailed" contain the results for the detailed compressor model described in Section 2. The first column in both tables indicates the nomination to be validated. By $\Delta_P \in \mathbb{R}^{|V_-|}$ with $\Delta_{P,u} := |P_u - \bar{P}_u|$ for all $u \in V_-$ we denote the difference in MW of the heat power P_u delivered to exit node u and the prescribed heat power demand $\bar{P}_u$. The maximum relative error is denoted by $\Delta_P^{\mathrm{rel}} \in \mathbb{R}^{|V_-|}$ with $\Delta_{P,u}^{\mathrm{rel}} := \Delta_{P,u}/\bar{P}_u$ for all $u \in V_-$. Finally, the remaining two columns contain the total number of ADM iterations (N) and the runtime of the ADM algorithm in seconds.

The algorithm terminates as soon as

- $|p_u - p'_u| < 1\,\mathrm{mbar}$ for all $u \in V_{\mathrm{cg}} \cap \bar{V}_{\mathrm{cg}}$,
- $|\sum_{a\in\delta^{\mathrm{out}}(u)} q_a - \sum_{a\in\delta^{\mathrm{in}}(u)} q_a| < 0.028\,\mathrm{kg\,s^{-1}}$ for all $u \in V_{\mathrm{cg}} \cap \bar{V}_{\mathrm{cg}}$,
- $|\sum_{a\in\mathcal{O}(u)}|P_a| - \sum_{a\in\mathcal{I}(u)}|P_a|| < 1\,\mathrm{kW}$ for all $u \in V_{\mathrm{cg}} \cap \bar{V}_{\mathrm{cg}}$,
- $|P_a - q_a H_{\mathrm{c},a}| < 1\,\mathrm{kW}$ for all $a \in A$,

and one of the following conditions for the power demands at the exits is fulfilled:

- $\|\Delta_P\|_\infty < 0.1\,\mathrm{MW}$,
- $\|\Delta_P\|_\infty < 0.5\,\mathrm{MW}$ and $\|\Delta_P^{\mathrm{rel}}\|_\infty < 0.08$, or
- $\|\Delta_P\|_\infty < 10\,\mathrm{MW}$ and $\|\Delta_P^{\mathrm{rel}}\|_\infty < 0.05$.

Note that, due to our modeling, the mixing equations (3e) and (3f) are always satisfied, so that these criteria are slight variations of the ones used in [13]. They are based on our experience with real-world instances from gas transport. To give a better overview of the relative performance of the methods, we also computed the relative increase in iteration count and runtime and also the time per iteration for each instance; see Table 6 and Table 7.

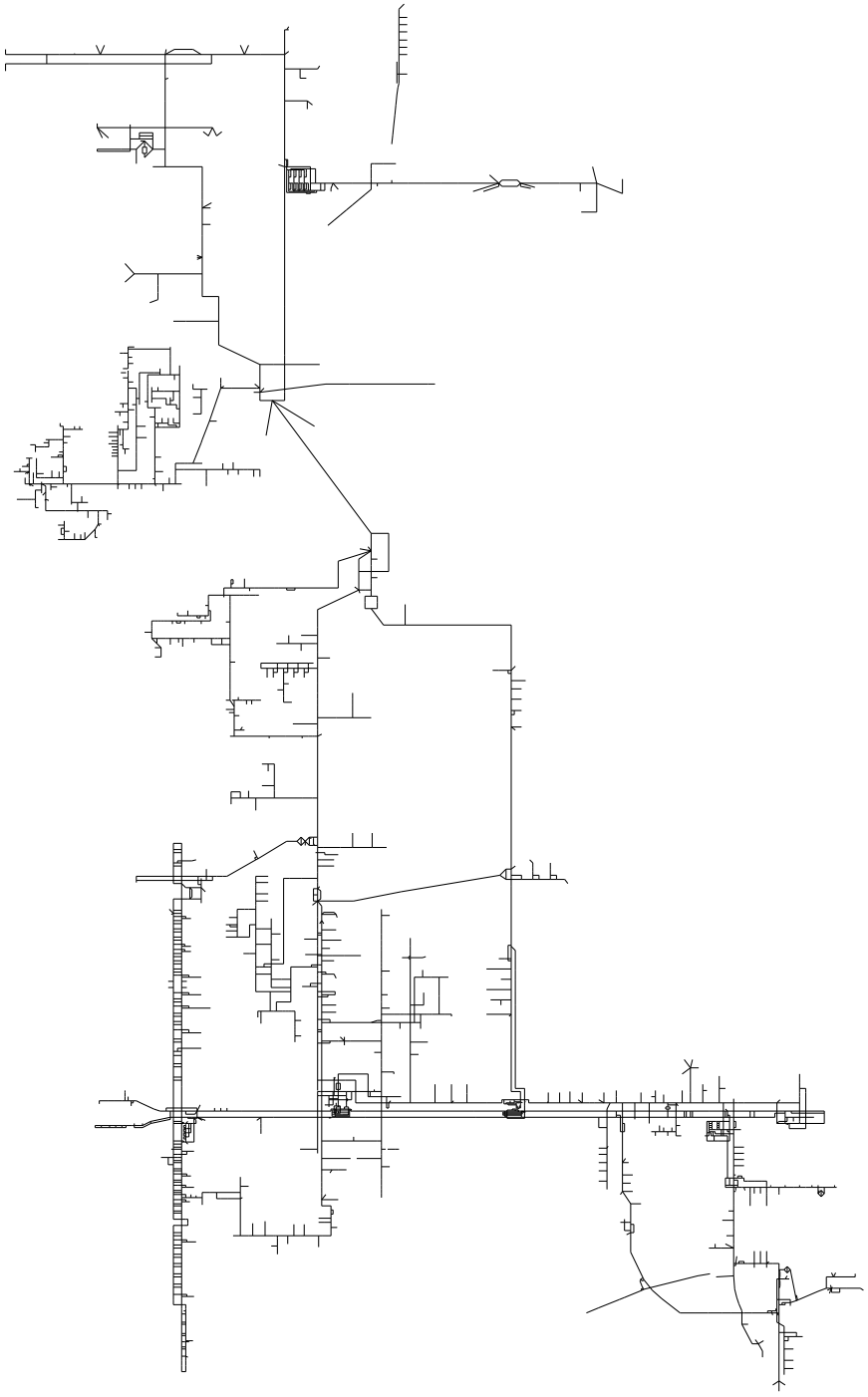

FIGURE 3. Schematic plot of the H-gas network.

TABLE 4. Results for the L-gas network with simplified and detailed compressor model.

	simplified				detailed			
Instance	$\|\Delta_P\|_\infty$	$\|\Delta_P^{\text{rel}}\|_\infty$	N	Time (s)	$\|\Delta_P\|_\infty$	$\|\Delta_P^{\text{rel}}\|_\infty$	N	Time (s)
L-01	1.79×10^{-1}	0.0109	3	4360	1.77×10^{-1}	0.0250	5	7158
L-02	1.52×10^{-2}	0.0000	5	3609	3.90×10^{-1}	0.0076	3	1911
L-03	3.57×10^{-1}	0.0110	2	1592	3.57×10^{-1}	0.0110	2	1188
L-04	1.61×10^{-1}	0.0020	3	6677	2.38×10^{-2}	0.0000	9	5242
L-05	4.88×10^{-1}	0.0125	4	4527	3.50×10^{-1}	0.0522	8	8726
L-06	2.07×10^{-1}	0.0076	3	2078	2.03×10^{-1}	0.0075	5	3781
L-07	1.52×10^{-2}	0.0000	3	1022	1.72×10^{-2}	0.0000	3	1610
L-08	5.46×10^{-1}	0.0035	3	2992	6.64×10^{-1}	0.0043	4	4115
L-09	4.02×10^{-2}	0.0000	3	4395	3.19×10^{-2}	0.0000	3	2230
L-10	1.29×10^{-1}	0.0021	3	4686	1.10×10^{-1}	0.0018	3	2838
L-11	7.43×10^{-2}	0.0000	3	3613	7.38×10^{-2}	0.0000	4	3262
L-12	1.23×10^{-2}	0.0000	3	3224	1.09×10^{-2}	0.0000	5	4297
L-13	2.04×10^{-2}	0.0000	3	3001	3.26×10^{-2}	0.0000	3	2131
L-14	9.25×10^{-1}	0.0555	2	1809	1.02×10^{-2}	0.0000	4	2123
L-15	6.04×10^{-2}	0.0000	3	2512	1.99×10^{-2}	0.0000	10	5508
L-16	1.23	0.0486	2	2535	1.09×10^{-2}	0.0000	4	3957
L-17	9.94×10^{-2}	0.0000	3	3138	1.11×10^{-2}	0.0000	5	2320
L-18	4.45×10^{-2}	0.0000	3	3075	5.68×10^{-2}	0.0000	3	2349
L-19	4.39×10^{-1}	0.0452	2	2272	6.67×10^{-2}	0.0000	3	2382
L-20	1.81	0.0476	2	1326	1.02×10^{-2}	0.0000	4	2006
L-21	3.49	0.0439	2	2365	1.35×10^{-2}	0.0000	4	2590
L-22	1.35×10^{-2}	0.0000	3	3576	5.43×10^{-2}	0.0000	3	2466
L-23	4.69×10^{-1}	0.0071	3	2560	2.12×10^{-2}	0.0000	3	2185
L-24	1.03×10^{-1}	0.0004	4	4279	1.12×10^{-2}	0.0000	5	4095
L-25	4.36×10^{-2}	0.0000	3	2993	9.29×10^{-2}	0.0000	6	4498
L-26	2.93	0.0501	2	1977	1.00×10^{-2}	0.0000	7	3081
L-27	3.18×10^{-1}	0.0522	4	4905	4.06×10^{-1}	0.0205	24	16 031
L-28	2.54×10^{-1}	0.0006	3	3091	7.65×10^{-2}	0.0000	5	4694

TABLE 5. Results for the H-gas network with simplified and detailed compressor model.

	simplified				detailed			
Instance	$\|\Delta_P\|_\infty$	$\|\Delta_P^{\text{rel}}\|_\infty$	N	Time (s)	$\|\Delta_P\|_\infty$	$\|\Delta_P^{\text{rel}}\|_\infty$	N	Time (s)
H-01-A	1.51×10^{-1}	0.0057	9	15 764	1.00×10^{-2}	0.0000	14	16 582
H-01-B	2.97×10^{-2}	0.0000	5	7085	3.25×10^{-1}	0.0039	13	16 040
H-01-C	2.97×10^{-2}	0.0000	5	6916	3.25×10^{-1}	0.0039	13	18 492
H-02-A	1.59	0.0169	7	10 175	1.15×10^{-1}	0.0000	56	70 469
H-02-B	1.12×10^{-2}	0.0000	7	10 116	1.35×10^{-2}	0.0000	11	17 895
H-02-C	1.43	0.0165	7	12 285	1.01×10^{-2}	0.0000	21	21 931
H-03-A	4.15	0.0529	3	6227	1.32	0.0015	10	8875
H-03-B	1.04×10^{-1}	0.0000	3	3065	1.22×10^{-2}	0.0000	7	5862
H-03-C	1.04×10^{-1}	0.0000	3	3134	1.22×10^{-2}	0.0000	7	7249
H-04-A	7.44	0.0465	9	16 842	7.93	0.0397	26	38 223
H-04-B	8.40	0.0192	11	14 427	8.47	0.0194	20	28 638
H-04-C	8.41	0.0192	18	16 114	8.42	0.0526	100	198 671
H-05-A	8.56	0.0397	12	26 281	6.79	0.0396	50	75 020
H-05-B	8.59	0.0196	14	22 346	8.59	0.0197	36	49 746
H-05-C	8.56	0.0229	35	69 074	8.61	0.0197	25	25 073
H-06-A	7.38	0.0461	4	7344	6.48	0.0405	31	46 936
H-06-B	8.82	0.0202	21	19 952	8.12	0.0186	26	25 258
H-06-C	8.31	0.0190	25	20 152	7.76	0.0485	14	13 394
H-07-A	1.75×10^{-1}	0.0001	7	12 406	1.02×10^{-2}	0.0000	11	14 432
H-07-B	1.62×10^{-2}	0.0000	19	42 141	2.93×10^{-2}	0.0000	21	20 117
H-07-C	1.38×10^{-1}	0.0021	11	19 134	3.34×10^{-1}	0.0226	34	38 685
H-08-A	3.48×10^{-2}	0.0000	18	55 170	1.06×10^{-2}	0.0000	31	36 914
H-08-B	1.34×10^{-2}	0.0000	11	27 953	4.15×10^{-2}	0.0000	75	105 896
H-08-C	7.38×10^{-1}	0.0043	9	18 140	1.13×10^{-2}	0.0000	96	101 174
H-09-A	4.99×10^{-1}	0.0139	4	6307	1.85×10^{-1}	0.0024	31	29 453
H-09-B	1.41	0.0056	9	18 116	1.07×10^{-2}	0.0000	9	10 104
H-09-C	1.71	0.0048	5	9592	1.01×10^{-2}	0.0000	11	8895
H-10-A	1.47	0.0195	7	14 800	2.21×10^{-1}	0.0002	12	16 828
H-10-B	1.15×10^{-2}	0.0000	21	48 784	1.14×10^{-2}	0.0000	30	41 337
H-10-C	1.36	0.0626	4	11 890	2.22×10^{-1}	0.0133	16	17 342

In the case of the L-gas network, all instances have been solved for both models by our method, i.e., the above given termination criteria are satisfied in all cases. Having a more detailed look at the results in Table 4, we see that the runtimes for both compressor models are in the same order of magnitude for all instances except for L-27. With the detailed compressor model, the runtimes increase by roughly 19 % in total and by roughly 10 % if we exclude the outlier L-27 (see Table 6). This is, however, a modest price to pay as we solve a far more detailed problem with additional nonlinear and nonconvex constraints. The median of the runtimes is almost the same in both cases: 2959 s for the simplified model and 3038 s for the detailed model. Interestingly, although the number of ADM iterations is in most cases higher for the detailed compressor model to achieve convergence, the average runtime of a single ADM iteration is lower in this case. This is because the solution does not change very much during the last few iterations with the detailed model and can be computed very fast.

For the H-gas network, all but one instances have been solved for both models. The only exception is instance H-04-C, for which the algorithm was not able to find a solution which is feasible for the detailed model, within the limit of 100 ADM iterations. The increase in runtime for the detailed model is more pronounced; see Table 5. On average, the runtime is roughly doubled compared to the simplified compressor model. This is mainly due to the fact that more iterations are needed to achieve convergence and can be explained with the fact that the number of compressor machines (104 in the H-gas network vs. 22 in the L-gas network) and the number of compressor groups (41 in the H-gas network vs. 12 in the L-gas network) is much higher in the H-gas network: The larger number of compressor groups leads to a larger number of penalty terms that have to be driven to zero by the penalty framework. Nevertheless, the increase in runtime is only sublinear in the number of compressors.

We note that the main obstacle to termination of the detailed model are tolerances corresponding to the compressor group penalty terms f_1, f_2, and f_3. Therefore, the other penalty terms f_4 and f_5 (concerning power and calorific value coupling) have typically lower values for the detailed model. For both networks it holds that the main amount of runtime is spent for solving the first-stage ADM model. Thus—although it is in general possible to parallelize the solution process of the second-stage ADM model—the overall runtime would only slightly benefit from it.

Finally, we would like to remark that in the solutions computed with the simplified compressor station model at least one compressor is operated outside its admissible working range for all of the above instances. The solutions computed with the detailed model thus strongly deviate from the solutions computed with the simplified model in terms of flow and pressure as well as in terms of discrete switching decisions.

In conclusion, the results show that our approach allows us to use a far more detailed compressor model while only incurring a modest increase in runtime. This shows that the penalty ADM approach can be worthwhile to pursue for problems with this or a similar structure.

5. Conclusion

In this paper we presented a highly detailed MINLP model of steady-state gas transport including both pooling effects, i.e., effects of mixing of different sorts of gas, and a comprehensive model of gas compressor stations hosting multiple compressor machines and drives. Solving such models on large-scale real-world gas transport networks was not possible before. We used tailored graph-based model reformulation techniques (extending the reformulations used in [13]) that yield block-separable MINLP structures. This made it possible to apply the penalty alternating direction

TABLE 6. Relative increase in iterations (N) and runtime (T) and time per iteration for the L-gas instances. Index "d" denotes the detailed model and index "s" denotes the simplified model.

Instance	$N_\mathrm{d}/N_\mathrm{s}$	$T_\mathrm{d}/T_\mathrm{s}$	$T_\mathrm{d}/N_\mathrm{d}$	$T_\mathrm{s}/N_\mathrm{s}$
L-01	1.67	1.64	1431.60	1453.33
L-02	0.60	0.53	637.00	721.80
L-03	1.00	0.75	594.00	796.00
L-04	3.00	0.79	582.44	2225.67
L-05	2.00	1.93	1090.75	1131.75
L-06	1.67	1.82	756.20	692.67
L-07	1.00	1.58	536.67	340.67
L-08	1.33	1.38	1028.75	997.33
L-09	1.00	0.51	743.33	1465.00
L-10	1.00	0.61	946.00	1562.00
L-11	1.33	0.90	815.50	1204.33
L-12	1.67	1.33	859.40	1074.67
L-13	1.00	0.71	710.33	1000.33
L-14	2.00	1.17	530.75	904.50
L-15	3.33	2.19	550.80	837.33
L-16	2.00	1.56	989.25	1267.50
L-17	1.67	0.74	464.00	1046.00
L-18	1.00	0.76	783.00	1025.00
L-19	1.50	1.05	794.00	1136.00
L-20	2.00	1.51	501.50	663.00
L-21	2.00	1.10	647.50	1182.50
L-22	1.00	0.69	822.00	1192.00
L-23	1.00	0.85	728.33	853.33
L-24	1.25	0.96	819.00	1069.75
L-25	2.00	1.50	749.67	997.67
L-26	3.50	1.56	440.14	988.50
L-27	6.00	3.27	667.96	1226.25
L-28	1.67	1.52	938.80	1030.33

method from [12] to solve the problems. We showed the practical relevance of our techniques by a computational study on Germany's largest gas transport networks. It turned out that the proposed method scales well with the size of the problem.

We think that the approach can be further refined and used both in the context of gas transport networks as well as for general mixed-integer nonlinear optimization. For the former, we plan to study general graph decompositions leading to different types of block-separability, where the connectedness of the decomposed parts of the graph determines the coupling of the MINLP blocks. This yields—as it is the case for the compressor station specific decomposition—much smaller subproblems that are then coordinated by a penalty framework. Finally, for general MINLPs it should be possible to automatically generate model reformulations yielding block-structured models that can be tackled with penalty ADMs.

ACKNOWLEDGMENTS

We acknowledge funding through the DFG SFB/Transregio 154, Subproject B07 and B08. The authors wish to thank all our collaborators from *ForNe – Research*

TABLE 7. Relative increase in iterations (N) and runtime (T) and time per iteration for the H-gas instances. Index "d" denotes the detailed model and index "s" denotes the simplified model.

Instance	$N_\mathrm{d}/N_\mathrm{s}$	$T_\mathrm{d}/T_\mathrm{s}$	$T_\mathrm{d}/N_\mathrm{d}$	$T_\mathrm{s}/N_\mathrm{s}$
H-01-A	1.56	1.05	1184.43	1751.56
H-01-B	2.60	2.26	1233.85	1417.00
H-01-C	2.60	2.67	1422.46	1383.20
H-02-A	8.00	6.93	1258.38	1453.57
H-02-B	1.57	1.77	1626.82	1445.14
H-02-C	3.00	1.79	1044.33	1755.00
H-03-A	3.33	1.43	887.50	2075.67
H-03-B	2.33	1.91	837.43	1021.67
H-03-C	2.33	2.31	1035.57	1044.67
H-04-A	2.89	2.27	1470.12	1871.33
H-04-B	1.82	1.99	1431.90	1311.55
H-04-C	5.56	12.33	1986.71	895.22
H-05-A	4.17	2.85	1500.40	2190.08
H-05-B	2.57	2.23	1381.83	1596.14
H-05-C	0.71	0.36	1002.92	1973.54
H-06-A	7.75	6.39	1514.06	1836.00
H-06-B	1.24	1.27	971.46	950.10
H-06-C	0.56	0.66	956.71	806.08
H-07-A	1.57	1.16	1312.00	1772.29
H-07-B	1.11	0.48	957.95	2217.95
H-07-C	3.09	2.02	1137.79	1739.45
H-08-A	1.72	0.67	1190.77	3065.00
H-08-B	6.82	3.79	1411.95	2541.18
H-08-C	10.67	5.58	1053.90	2015.56
H-09-A	7.75	4.67	950.10	1576.75
H-09-B	1.00	0.56	1122.67	2012.89
H-09-C	2.20	0.93	808.64	1918.40
H-10-A	1.71	1.14	1402.33	2114.29
H-10-B	1.43	0.85	1377.90	2323.05
H-10-C	4.00	1.46	1083.88	2972.50

Cooperation Network Optimization and especially our former industry partner, Open Grid Europe GmbH, for their support and the provision of the network data. This research has been performed as part of the Energie Campus Nürnberg and supported by funding through the "Aufbruch Bayern (Bavaria on the move)" initiative of the state of Bavaria, and the German Ministry of Education and Research under project number 02WER1323A. Finally, we thank Benjamin Hiller for many fruitful discussions on the topic of this paper and an anonymous reviewer whose detailed comments greatly helped to improve the quality of the article.

REFERENCES

[1] B. T. Baumrucker, J. G. Renfro, and L. T. Biegler. "MPEC problem formulations and solution strategies with chemical engineering applications." In: *Computers & Chemical Engineering* (2008), pp. 2903–2913. DOI: 10.1016/j.compchemeng.2008.02.010.

[2] D. P. Bertsekas and J. N. Tsitsiklis. *Parallel and Distributed Computation: Numerical Methods*. Upper Saddle River, NJ, USA: Prentice-Hall, Inc., 1989. URL: http://hdl.handle.net/1721.1/3719.

[3] S. Boyd, N. Parikh, E. Chu, B. Peleato, and J. Eckstein. "Distributed Optimization and Statistical Learning via the Alternating Direction Method of Multipliers." In: *Found. Trends Mach. Learn.* 3.1 (Jan. 2011), pp. 1–122. DOI: 10.1561/2200000016.

[4] P. Domschke, B. Geißler, O. Kolb, J. Lang, A. Martin, and A. Morsi. "Combination of Nonlinear and Linear Optimization of Transient Gas Networks." In: *INFORMS Journal on Computing* 23.4 (2011), pp. 605–617. DOI: 10.1287/ijoc.1100.0429.

[5] A. Fügenschuh, B. Geißler, R. Gollmer, A. Morsi, M. E. Pfetsch, J. Rövekamp, M. Schmidt, K. Spreckelsen, and M. C. Steinbach. "Physical and technical fundamentals of gas networks." In: *Evaluating Gas Network Capacities*. Ed. by T. Koch, B. Hiller, M. E. Pfetsch, and L. Schewe. SIAM-MOS series on Optimization. SIAM, 2015. Chap. 2, pp. 17–43. DOI: 10.1137/1.9781611973693.ch2.

[6] D. Gabay and B. Mercier. "A dual algorithm for the solution of nonlinear variational problems via finite element approximation." In: *Computers & Mathematics with Applications* 2.1 (1976), pp. 17–40. DOI: 10.1016/0898-1221(76)90003-1.

[7] B. Geißler, O. Kolb, J. Lang, G. Leugering, A. Martin, and A. Morsi. "Mixed Integer Linear Models for the Optimization of Dynamical Transport Networks." In: *Mathematical Methods of Operations Research* 73.3 (2011), pp. 339–362. DOI: 10.1007/s00186-011-0354-5.

[8] B. Geißler. "Towards Globally Optimal Solutions for MINLPs by Discretization Techniques with Applications in Gas Network Optimization." PhD thesis. Friedrich-Alexander-Universität Erlangen-Nürnberg (FAU), 2011.

[9] B. Geißler, A. Martin, A. Morsi, and L. Schewe. "The MILP-relaxation approach." In: *Evaluating Gas Network Capacities*. Ed. by T. Koch, B. Hiller, M. E. Pfetsch, and L. Schewe. SIAM-MOS series on Optimization. SIAM, 2015. Chap. 6, pp. 103–122. DOI: 10.1137/1.9781611973693.ch6.

[10] B. Geißler, A. Martin, A. Morsi, and L. Schewe. "Using Piecewise Linear Functions for Solving MINLPs." In: *Mixed Integer Nonlinear Programming*. Ed. by J. Lee and S. Leyffer. Vol. 154. The IMA Volumes in Mathematics and its Applications. Springer New York, 2012, pp. 287–314. DOI: 10.1007/978-1-4614-1927-3_10.

[11] B. Geißler, A. Morsi, and L. Schewe. "A New Algorithm for MINLP Applied to Gas Transport Energy Cost Minimization." In: *Facets of Combinatorial Optimization*. Ed. by M. Jünger and G. Reinelt. Berlin, Heidelberg: Springer, 2013, pp. 321–353. DOI: 10.1007/978-3-642-38189-8_14.

[12] B. Geißler, A. Morsi, L. Schewe, and M. Schmidt. *Penalty Alternating Direction Methods for Mixed-Integer Optimization: A New View on Feasibility Pumps*. Apr. 2016. URL: http://www.optimization-online.org/DB_HTML/2016/04/5399.html. Submitted.

[13] B. Geißler, A. Morsi, L. Schewe, and M. Schmidt. "Solving power-constrained gas transportation problems using an MIP-based alternating direction method." In: *Computers & Chemical Engineering* 82 (2015), pp. 303–317. DOI: 10.1016/j.compchemeng.2015.07.005.

[14] R. Glowinski and A. Marroco. "Sur l'approximation, par éléments finis d'ordre un, et la résolution, par pénalisation-dualité d'une classe de problèmes de Dirichlet non linéaires." In: *ESAIM: Mathematical Modelling and Numerical*

Analysis - Modélisation Mathématique et Analyse Numérique 9.R2 (1975), pp. 41–76. URL: http://eudml.org/doc/193269.

[15] J. Gorski, F. Pfeuffer, and K. Klamroth. "Biconvex sets and optimization with biconvex functions: a survey and extensions." In: *Mathematical Methods of Operations Research* 66.3 (2007), pp. 373–407. DOI: 10.1007/s00186-007-0161-1.

[16] Gurobi Optimization, Inc. *Gurobi Optimizer Reference Manual*. 2015. URL: http://www.gurobi.com.

[17] S.-P. Han and O. L. Mangasarian. "Exact penalty functions in nonlinear programming." In: *Mathematical Programming* 17.1 (1979), pp. 251–269. DOI: 10.1007/BF01588250.

[18] M. Jünger and G. Reinelt, eds. *Facets of Combinatorial Optimization*. Berlin, Heidelberg: Springer, 2013. DOI: 10.1007/978-3-642-38189-8.

[19] T. Koch, B. Hiller, M. E. Pfetsch, and L. Schewe, eds. *Evaluating Gas Network Capacities*. SIAM-MOS series on Optimization. SIAM, 2015. xvii + 364. DOI: 10.1137/1.9781611973693.

[20] *LaMaTTO++: A Framework for Modeling and Solving Mixed-Integer Nonlinear Programming Problems on Networks*. http://www.mso.math.fau.de/edom/projects/lamatto.html. 2016.

[21] D. Mahlke, A. Martin, and S. Moritz. "A Mixed Integer Approach for Time-Dependent Gas Network Optimization." In: *Optimization Methods and Software* 25.4 (2010), pp. 625–644.

[22] A. Martin, M. Möller, and S. Moritz. "Mixed Integer Models for the Stationary Case of Gas Network Optimization." In: *Mathematical Programming, Series B* 105.2 (2006), pp. 563–582.

[23] B. A. McCarl. *GAMS User Guide*. VERSION 23.0. 2009.

[24] A. Morsi. "Solving MINLPs on Loosely-Coupled Networks with Applications in Water and Gas Network Optimization." PhD thesis. Friedrich-Alexander-Universität Erlangen-Nürnberg (FAU), 2013.

[25] J. Nocedal and S. J. Wright. *Numerical Optimization*. 2nd ed. Springer Series in Operations Research and Financial Engineering. New York: Springer Verlag, 2006. DOI: 10.1007/978-0-387-40065-5.

[26] I. Nowak. *Relaxation and decomposition methods for mixed integer nonlinear programming*. 2005. URL: urn:nbn:de:kobv:11-10038479.

[27] M. E. Pfetsch, A. Fügenschuh, B. Geißler, N. Geißler, R. Gollmer, B. Hiller, J. Humpola, T. Koch, T. Lehmann, A. Martin, A. Morsi, J. Rövekamp, L. Schewe, M. Schmidt, R. Schultz, R. Schwarz, J. Schweiger, C. Stangl, M. C. Steinbach, S. Vigerske, and B. M. Willert. "Validation of nominations in gas network optimization: models, methods, and solutions." In: *Optimization Methods and Software* 30.1 (2015), pp. 15–53. DOI: 10.1080/10556788.2014.888426.

[28] R. Z. Ríos-Mercado and C. Borraz-Sánchez. "Optimization problems in natural gas transportation systems: A state-of-the-art review." In: *Applied Energy* 147 (2015), pp. 536–555. DOI: 10.1016/j.apenergy.2015.03.017.

[29] D. Rose, M. Schmidt, M. C. Steinbach, and B. M. Willert. "Computational optimization of gas compressor stations: MINLP models versus continuous reformulations." In: *Mathematical Methods of Operations Research* 83.3 (2016), pp. 409–444. DOI: 10.1007/s00186-016-0533-5.

[30] N. V. Sahinidis. *BARON 14.3.1: Global Optimization of Mixed-Integer Nonlinear Programs,* User's Manual. 2014.

[31] L. Schewe, T. Koch, A. Martin, and M. E. Pfetsch. "Mathematical optimization for evaluating gas network capacities." In: *Evaluating Gas Network Capacities*. Ed. by T. Koch, B. Hiller, M. E. Pfetsch, and L. Schewe.

SIAM-MOS series on Optimization. SIAM, 2015. Chap. 5, pp. 87–102. DOI: 10.1137/1.9781611973693.ch5.

[32] M. Schmidt. "A Generic Interior-Point Framework for Nonsmooth and Complementarity Constrained Nonlinear Optimization." PhD thesis. Gottfried Wilhelm Leibniz Universität Hannover, 2013.

[33] M. Schmidt, M. C. Steinbach, and B. M. Willert. "A Primal Heuristic for Nonsmooth Mixed Integer Nonlinear Optimization." In: *Facets of Combinatorial Optimization*. Ed. by M. Jünger and G. Reinelt. Berlin, Heidelberg: Springer, 2013, pp. 295–320. DOI: 10.1007/978-3-642-38189-8_13.

[34] M. Schmidt, M. C. Steinbach, and B. M. Willert. "An MPEC based heuristic." In: *Evaluating Gas Network Capacities*. Ed. by T. Koch, B. Hiller, M. E. Pfetsch, and L. Schewe. SIAM-MOS series on Optimization. SIAM, 2015. Chap. 9, pp. 163–179. DOI: 10.1137/1.9781611973693.ch9.

[35] M. Schmidt, M. C. Steinbach, and B. M. Willert. "High detail stationary optimization models for gas networks." In: *Optimization and Engineering* 16.1 (2015), pp. 131–164. DOI: 10.1007/s11081-014-9246-x.

[36] M. Schmidt, M. C. Steinbach, and B. M. Willert. "High detail stationary optimization models for gas networks: validation and results." In: *Optimization and Engineering* 17.2 (2016), pp. 437–472. DOI: 10.1007/s11081-015-9300-3.

[37] M. Tawarmalani and N. V. Sahinidis. "A polyhedral branch-and-cut approach to global optimization." In: *Math. Program.* 103.2 (2005), pp. 225–249. DOI: 10.1007/s10107-005-0581-8.

[38] T. van der Hoeven. "Math in Gas and the Art of Linearization." PhD thesis. Rijksuniversiteit Groningen, 2004.

[39] R. E. Wendell and A. P. Hurter Jr. "Minimization of a non-separable objective function subject to disjoint constraints." In: *Operations Research* 24.4 (1976), pp. 643–657. DOI: 10.1287/opre.24.4.643.

[1]Björn Geissler, Antonio Morsi, Lars Schewe, Friedrich-Alexander-Universität Erlangen-Nürnberg (FAU), Discrete Optimization, Cauerstr. 11, 91058 Erlangen, Germany, [2]Martin Schmidt, (a) Friedrich-Alexander-Universität Erlangen-Nürnberg (FAU), Discrete Optimization, Cauerstr. 11, 91058 Erlangen, Germany; (b) Energie Campus Nürnberg, Fürther Str. 250, 90429 Nürnberg, Germany

E-mail address: [1]{bjoern.geissler,antonio.morsi,lars.schewe}@fau.de

E-mail address: [2]mar.schmidt@fau.de